

## XPS Investigation of Strong Metal-Support Interactions on Group IIIa-Va Oxides

B. A. SEXTON, A. E. HUGHES, AND K. FOGER

CSIRO Division of Materials Science, Catalysis and Surface Science Laboratory, University of Melbourne, Parkville, 3052, Victoria, Australia

Received December 11, 1981; revised March 2, 1982

X-Ray photoelectron spectroscopy (XPS) has been used to measure the core level electron binding energies of Rh and Pt supported on Group IIIa-Va oxides after low (200°C) and high (550°C) temperature reductions. For 2% Rh/TiO<sub>2</sub> we observe a small, reversible chemical shift ( $\Delta E_B = -0.2 \pm 0.05$  eV) for the Rh 3d  $\frac{5}{2}$  peak indicating some electron transfer from Ti<sup>3+</sup> to rhodium. This small value is in contrast to the large initial splitting of -0.6 eV which we found was due mostly to sintering of the rhodium during the initial reductions. At least one oxidation and reduction cycle was needed before a stable reversible set of binding energies was obtained. We estimate that the -0.2 eV value is a lower limit on the chemical shift, since there may be differences in the extra-atomic relaxation effects for the 200 and 550°C catalysts due to a reversible change in the particle size or morphology. Further sputtering experiments on the pure oxides were used to disclose the nature of the surface species likely to cause the SMSI electron transfer. These were found to be Ti<sup>3+</sup> (TiO<sub>2</sub>), Nb<sup>2-4+</sup> (Nb<sub>2</sub>O<sub>5</sub>), Ta<sup>2-4+</sup> (Ta<sub>2</sub>O<sub>5</sub>), and V<sup>2+</sup> (V<sub>2</sub>O<sub>3</sub>). These reduced cations were readily oxidized in air at room temperature back to the stoichiometric oxide.

### 1. INTRODUCTION

A strong metal support interaction (SMSI) effect has been reported by Tauster *et al.* (1, 2) and Baker *et al.* (3) for the Pt/TiO<sub>2</sub> system. Suppression of CO and H<sub>2</sub> chemisorption after high-temperature reduction at 500°C is believed to be related to interaction of Pt atoms and clusters with Ti<sup>3+</sup> defects (4). In the currently accepted theory, Horsley (4) has predicted a significant charge transfer of up to 0.6 electrons per atom donated to platinum, resulting in a Ptδ<sup>-</sup> state. It is this entity which is presumed to cause the suppression of chemisorption (1-3) and changes in catalyst selectivity during reactions on reduced catalysts. It is not clear at this present stage what the effects of charge transfer into small platinum clusters might be, since the model of Tauster, Baker, and Horsley (1-4) assumes that the metal clusters form monolayer "rafts" after high-temperature reduction. In this model, maximum interaction of each Pt atom with the Ti<sup>3+</sup> states would oc-

cur, although detailed electron microscopy studies have not conclusively verified the presence of "rafts."

The question of how much electron transfer occurs when noble metals are reduced on SMSI oxides may be answered by XPS. XPS core level binding energies reflect the oxidation state of the metal atoms. Although negative oxidation states of noble metal atoms are rare, one can predict the approximate chemical shift of 1 eV per electron per atom based on the positive oxidation states (5). Initial work with XPS has been done by Chung's (6, 7) group with model Pt/SrTiO<sub>3</sub> and Ni/TiO<sub>2</sub> films. Chung separated the relaxation shifts from the electron transfer, or "chemical shift" by varying the amount of platinum and nickel on the SrTiO<sub>3</sub> and TiO<sub>2</sub> films. A value of around 0.6e<sup>-</sup> per atom transferred to platinum was found for the highly dispersed, low coverage phase of Pt/SrTiO<sub>3</sub> (6). More recently, Haller (8) has observed small chemical shifts of ~0.2 eV to lower binding energy for a Rh/TiO<sub>2</sub> catalyst after high-

temperature reduction. Haller (8) also found that initial sintering of the catalyst during the first few high-temperature heating cycles changed the binding energy of the Rh significantly, and had to be separated from the actual chemical shift due to interaction with defects. A recent paper by Fung (9) reports a large ( $-1.6$  eV) shift in the Pt 4f  $7/2$  level between unreduced and high-temperature reduced Pt/TiO<sub>2</sub> films. Fung was unable, however, to separate the chemical shift from the extra-atomic relaxation shift due to particle size differences.

The purpose of this work was to examine in more detail the measurements of Haller (8) on a Rh/TiO<sub>2</sub> catalyst, and examine the general question of the nature of defects on group IIIa–Va oxides. We identify the low-valence states by sputtering and separate the reducible and nonreducible oxides. On comparing catalysts of Rh and Pt supported on both reducible and nonreducible oxides we see large initial binding energy shifts on most of the reducible oxides after high-temperature reduction. Finally, we examine the system Rh/TiO<sub>2</sub> in detail, separate the relaxation shift contributions due to initial sintering, and set a lower limit on the chemical shift due to electron transfer to rhodium.

## 2. EXPERIMENTAL

XPS measurements were taken on a Vacuum Generators Escalab 5 Spectrometer with a sample entry lock and a preparation chamber. Unreduced catalysts and oxides were either pressed into thin 12-mm discs or dispersed on the surface of stainless-steel sample holders. Catalysts were prepared by impregnation of the pure oxides with solutions of RhCl<sub>3</sub> or H<sub>2</sub>PtCl<sub>6</sub>. The pure oxides (CERAC) were not pretreated, prior to the sputtering experiments. Reduction and oxidation of the samples were done in the sample preparation chamber, where hydrogen or oxygen was admitted to a static pressure of 50–100 Torr and the samples were heated by conduction on a P8 sample probe. After reduction or oxidation,

the samples were transferred directly from the evacuated preparation chamber into the analysis chamber. This procedure eliminated exposure to air.

XPS measurements were taken with MgK $\alpha$  radiation (150 W) and the spectrometer run at 35 eV pass energy (4-mm slits). Line half-widths of the XPS peaks were approximately 1.5 eV. Due to the inherent charging of each sample, and the variation of charging with oxidation or reduction, the metal lines were referenced to a main oxide line (e.g., Ti 2p  $3/2$  at 459.0 eV). These lines were not affected by the pretreatments and allowed the binding energy variations of the metal lines to be measured to  $\pm 0.05$  eV.

Sputtering experiments were carried out on the oxide supports to locally reduce the surfaces of the reducible oxides (Ta<sub>2</sub>O<sub>5</sub>, V<sub>2</sub>O<sub>3</sub>, Nb<sub>2</sub>O<sub>5</sub>, TiO<sub>2</sub>) and allow identification of the defect states. Each oxide was sputtered for 10 min with 5000 eV Ar<sup>+</sup> ions (50  $\mu$ A). These surfaces were then examined with XPS and then exposed to air to test the stability of the defect surface states toward oxidation.

## 3. RESULTS

### 3.1 Reduction of Group III–Va Oxides in Hydrogen

Each of the six oxides TiO<sub>2</sub>, V<sub>2</sub>O<sub>3</sub>, Nb<sub>2</sub>O<sub>5</sub>, Ta<sub>2</sub>O<sub>5</sub>, Y<sub>2</sub>O<sub>3</sub>, and HfO<sub>2</sub> was examined with XPS in the unreduced (as received) state, and after reduction in hydrogen at 50 Torr pressure at 200 and 550°C. The reduction time for each case was 10 min. Scans of the following levels were made to determine the presence of any surface reduction: Ti 2p, V 3d, Nb 3d, Ta 4f, Y 3d, and Hf 4f. With the exception of V<sub>2</sub>O<sub>3</sub> after reduction at 550°C, no evidence was found for the presence of lower valence state surface defects, indicating that insignificant (<5%) surface reduction had occurred. Although color changes of TiO<sub>2</sub> (white  $\rightarrow$  blue), occurred at 550°C indicating bulk Ti<sup>3+</sup>, we found insignificant amounts (<5%) of Ti<sup>3+</sup> in the XPS.

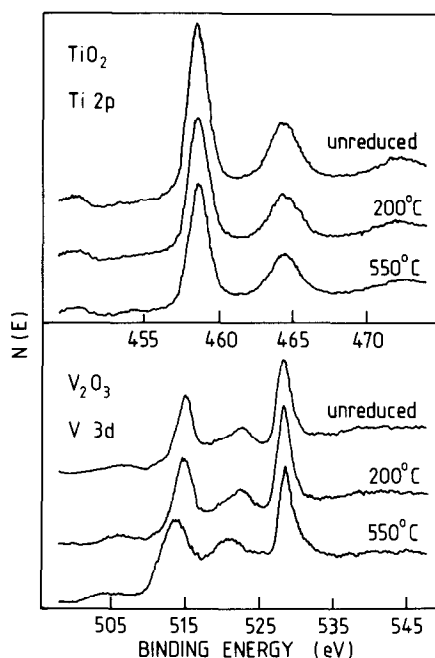


FIG. 1. XPS of the Ti 2p and V 3d regions for the oxides as received, and after reduction in 50 Torr  $H_2$  at 200 and 550°C. Some reduction of the  $V_2O_3$  occurred at 550°C. The peak near 530 eV in the  $V_2O_3$  spectrum is the O 1s level.

The results are summarized in Fig. 1 for  $TiO_2$  and  $V_2O_3$  and listed in Table 1 for the other oxides. Within the limits of detectability of the XPS technique ( $\sim 5\%$ ) only the

Oxide	Oxidation states present		After sputtering <sup>b</sup>
	200°C	550°C	
$TiO_2$	$Ti^{4+}$	$Ti^{4+}$	$Ti^{4+}$ , $Ti^{3+}$
$V_2O_3$	$V^{3+}$	$V^{3+}$ , ( $V^{2+}$ )	$V^{3+}$ , $V^{2+}$
$Nb_2O_5$	$Nb^{5+}$	$Nb^{5+}$	$Nb^{5+}$ , $Nb^{2-4+}$
$Ta_2O_5$	$Ta^{5+}$	$Ta^{5+}$	$Ta^{5+}$ , $Ta^{2-4+}$
$HfO_2$	$Hf^{4+}$	$Hf^{4+}$	$Hf^{4+}$
$Y_2O_3$	$Y^{3+}$	$Y^{3+}$	$Y^{3+}$

<sup>a</sup> Oxides reduced for 10 min in 50 Torr  $H_2$  at the appropriate temperature, then transferred *in situ* to the XPS chamber.

<sup>b</sup> Sputtered with  $Ar^+$  (50  $\mu A$ , 10 min, 5 kV ions). Then transferred to XPS chamber without air exposure.

stoichiometric valence states were observed at the surfaces of the oxides with reduction temperatures up to 550°C.

### 3.2 Surface Reduction of the Oxides with an Ion Beam

To identify possible lower valence state surface defects which may participate in the SMSI effect, we sputtered the surfaces of the oxides with an  $Ar^+$  ion gun and monitored the surface oxidation states with XPS. Sputtering is known to cause local surface reduction by preferential removal of oxygen from the surface layer. The results are shown for  $TiO_2$ ,  $Nb_2O_5$ , and  $Ta_2O_5$  in Figs. 2–4 and the other oxides listed in Table 1. After sputtering, we found significant surface reduction on the surfaces of  $TiO_2$ ,  $Nb_2O_5$ ,  $Ta_2O_5$ , and  $V_2O_3$ , with an insignificant amount of reduction on the oxides  $HfO_2$ ,  $Y_2O_3$ . The oxides therefore divide up into two groups: reducible and non-reducible, which correlates with the thermodynamic reducibility as mentioned by Tauster (1) in the early SMSI work. Specifically, the valence states positively identified by the XPS chemical shifts on each oxide surface after sputtering are as follows:  $TiO_2$  ( $Ti^{4+}$ ,  $Ti^{3+}$ ),  $Nb_2O_5$  ( $Nb^{5+}$ ,

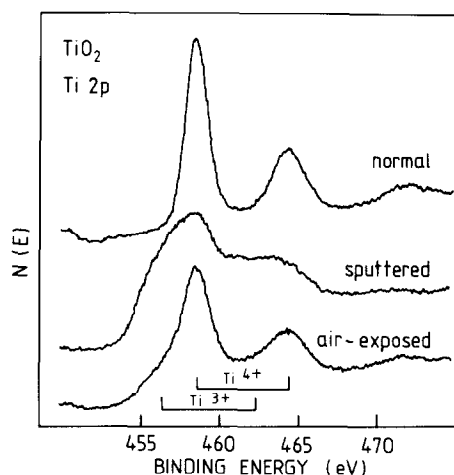


FIG. 2.  $TiO_2$  (anatase) XPS showing the Ti 2p region after sputtering and after exposure to air.  $Ti^{3+}$  states are generated and rapidly reoxidize to  $Ti^{4+}$  after air exposure.

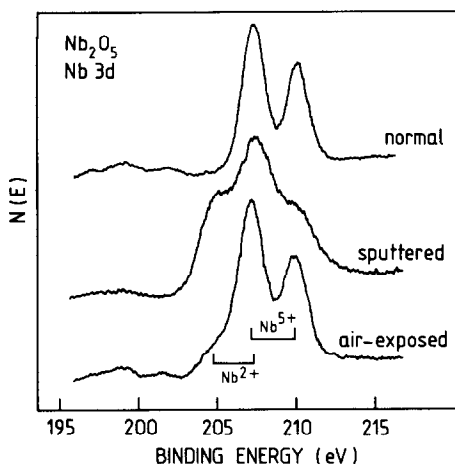


Fig. 3.  $\text{Nb}_2\text{O}_5$  XPS showing Nb 3d region after sputtering and then exposure to air.  $\text{Nb}^{2+}$  states are positively identified, but  $\text{Nb}^{3+}$  and  $\text{Nb}^{4+}$  may also be present. Air exposure rapidly reoxidizes these states back to  $\text{Nb}^{5+}$ .

$\text{Nb}^{2+}$ ),  $\text{Ta}_2\text{O}_5$  ( $\text{Ta}^{5+}$ ,  $\text{Ta}^{2+}$ ),  $\text{V}_2\text{O}_3$  ( $\text{V}^{3+}$ ,  $\text{V}^{2+}$ ),  $\text{HfO}_2$  ( $\text{Hf}^{4+}$ ), and  $\text{Y}_2\text{O}_3$  ( $\text{Y}^{3+}$ ). For  $\text{Nb}_2\text{O}_5$  and  $\text{Ta}_2\text{O}_5$  intermediate oxidation states were probably present but were not easily separated due to the limited XPS resolution.

Positive identification of these lower valence state defects has already been made for  $\text{TiO}_2$  by Henrich *et al.* (10) where sputtering was used to form a high concentration of surface  $\text{Ti}^{3+}$ .

Although the reducing conditions in an  $\text{Ar}^+$  ion beam are far more severe than heating in molecular  $\text{H}_2$ , the ready formation of the low valence surface states on  $\text{TiO}_2$ ,  $\text{Nb}_2\text{O}_5$ ,  $\text{Ta}_2\text{O}_5$ , and  $\text{V}_2\text{O}_3$  suggests that such states may be formed by hydrogen spillover from supported metals (11). At this point, however, it suffices to prove that defect states exist at the surface under strongly reducing conditions, but are not present on the more refractory oxides ( $\text{Y}_2\text{O}_3$ ,  $\text{HfO}_2$ ).

To test the stability of the defect states on  $\text{TiO}_2$ ,  $\text{Nb}_2\text{O}_5$ ,  $\text{Ta}_2\text{O}_5$ , and  $\text{V}_2\text{O}_3$  toward reoxidation, we exposed the sputtered surfaces to air for a few seconds, and then reintroduced them to the analysis chamber. The results are shown in Figs. 2–4 (lower curve;

air-exposed). In all cases, the low binding energy features in the spectra were considerably attenuated and the normal stoichiometric spectrum restored. We interpret these observations as the reoxidation of the low valence states ( $\text{Ti}^{3+}$ ,  $\text{Nb}^{2+}$ ,  $\text{Ta}^{2+}$ ,  $\text{V}^{2+}$ ) to the stoichiometric surface layer states ( $\text{Ti}^{4+}$ ,  $\text{Nb}^{5+}$ ,  $\text{Ta}^{5+}$ ,  $\text{V}^{3+}$ ) with incorporation of oxygen into the surface layer.

A conclusion about low valence states on the surfaces of the group IIIa–Va oxides may now be drawn. These oxides fall into two groups: reducible ( $\text{Ta}_2\text{O}_5$ ,  $\text{TiO}_2$ ,  $\text{V}_2\text{O}_3$ ,  $\text{Nb}_2\text{O}_5$ ) and nonreducible ( $\text{HfO}_2$ ,  $\text{Y}_2\text{O}_3$ ). Heating in hydrogen at temperatures up to  $550^\circ\text{C}$  does not cause observable reduction at the surface of these oxides to any significant extent (with the exception of  $\text{V}_2\text{O}_3$  at  $550^\circ\text{C}$ ). It should be pointed out, however, that the ion/vacancy mobility at  $550^\circ\text{C}$  is high and the reduced ions are usually more stable in the bulk (15). Surface reduction may be occurring at  $550^\circ\text{C}$ , but the resulting surface concentration of reduced ions may be quite small (15).

Reduction of the oxide surfaces with  $\text{Ar}^+$  induces low oxidation states on the reducible oxide surfaces, and these states are un-

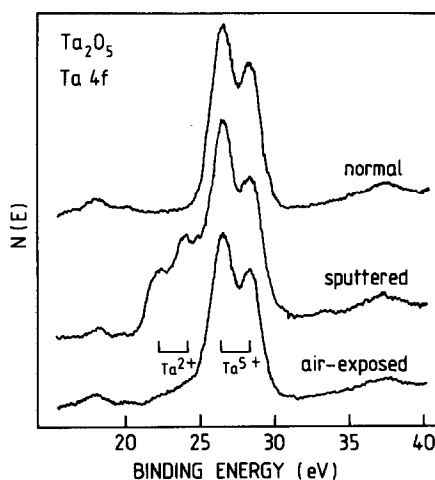


Fig. 4.  $\text{Ta}_2\text{O}_5$  XPS showing Ta 4f region after sputtering and then exposure to air.  $\text{Ta}^{2+}$  states are positively identified but  $\text{Ta}^{3+}$  and  $\text{Ta}^{4+}$  may also be present. Air exposure rapidly reoxidizes these states back to  $\text{Ta}^{5+}$ .

stable in the presence of oxygen and reoxidize rapidly back to the stoichiometric surface layer. It is important to characterize the oxide surfaces prior to measuring the supported catalysts, because these defects states are believed to play a role in electron transfer to the supported particles (4). Evidence for this will be given in the next section.

### 3.3 XPS Measurements of Binding Energies of Supported Rh and Pt on Group IIIa-Va Oxides

Six catalysts were prepared (1% Pt/TiO<sub>2</sub>, 2% Rh/TiO<sub>2</sub>, 1% Rh/Ta<sub>2</sub>O<sub>5</sub>, 1% Rh/Nb<sub>2</sub>O<sub>5</sub>, and 1% Rh/HfO<sub>2</sub>) by normal impregnation techniques and reduced *in situ* in the ESCALAB preparation chamber. Two temperatures, 200 and 550°C, were chosen to correspond to the "active" (200°C) and de-

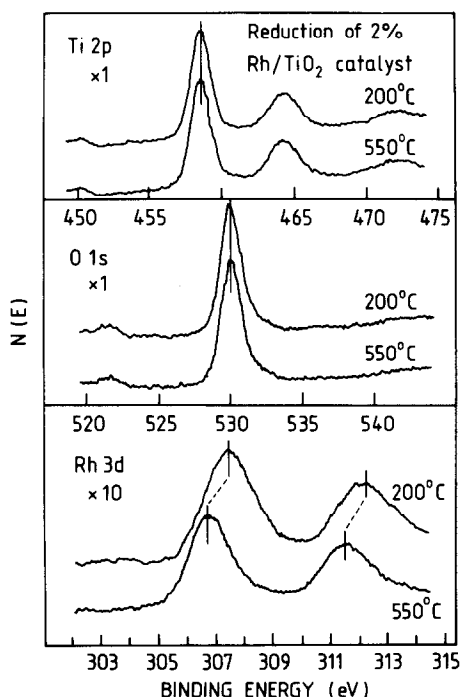


FIG. 5. XPS of the 2% Rh/TiO<sub>2</sub> catalyst showing the Ti 2p, O 1s, and Rh 3d lines after an initial low- (200°C) and high- (550°C) temperature reduction. After correcting the Ti 2p and O 1s levels for charging, a negative ( $-0.6 \pm 0.05$ ) eV shift is seen in the Rh 3d levels after high-temperature reduction.

TABLE II

Catalyst	$\Delta E_B^a$ (200–550°C)
1% Pt/TiO <sub>2</sub>	$-0.4 \pm 0.05$ eV
2% Rh/TiO <sub>2</sub>	$-0.6^b$
1% Rh/V <sub>2</sub> O <sub>3</sub>	$-0.3$
1% Rh/Ta <sub>2</sub> O <sub>5</sub>	0
1% Rh/Nb <sub>2</sub> O <sub>5</sub>	$-0.3$
1% Rh/HfO <sub>2</sub>	0

<sup>a</sup> Pt 4f 7/2 peak or Rh 3d 5/2 binding energy. This shift is for the *first* reduction at the stated temperature.

<sup>b</sup> This catalyst had an average particle size of 1.5 nm (15 Å) after an initial sintering (reduction-oxidation cycle) and temperature-programmed reduction to 550°C, as determined by electron microscopy. The catalyst was exposed to air prior to the electron microscopy measurement, and was the most highly dispersed of the group (>75% dispersion).

activated (550°C) states as observed by Tauster (1, 2), Baker (3), and others (12). Reduction was effected within a few seconds at both temperatures, and was done for 5–10 min to ensure completion of the process.

Binding energies of the Rh 3d 5/2 and Pt 4f 7/2 peaks near 307 and 71.3 eV, respectively, were measured after referencing these lines to the main metal line in the oxide. This procedure compensated for charging. We then measured the shift in the binding energy of the Rh or Pt peak at 550°C relative to the 200°C case. A negative shift,  $\Delta E$ , would correspond to electron transfer into the Rh or Pt atoms from the support, as predicted by Horsley (4), provided that no significant particle size change occurred between the two temperatures (relaxation energy difference).

The results are shown in Fig. 5 for Rh/TiO<sub>2</sub> and Table 2, comparing the initial 200°C reduction with the initial 550°C reduction. Four considerable negative shifts were observed on Pt/TiO<sub>2</sub>, Rh/TiO<sub>2</sub>, Rh/V<sub>2</sub>O<sub>3</sub>, and Rh/Nb<sub>2</sub>O<sub>5</sub> with little or no shift on Ta<sub>2</sub>O<sub>5</sub> and HfO<sub>2</sub>. With the exception of Ta<sub>2</sub>O<sub>5</sub>, this is the expected result for elec-

tron transfer into the Pt or Rh supported on the reducible oxides. An even larger negative shift of  $-1.6$  eV was observed by Fung (9) for initial reduction of a model Pt/TiO<sub>2</sub> catalyst at these two temperatures.

Further experiments showed, however, that most of these negative shifts may be explained by an initial sintering of the particles at 550°C, causing a considerable relaxation shift (increasing particle size). Such an effect was investigated in detail for the 2% Rh/TiO<sub>2</sub> catalyst which showed the largest initial splitting of  $-0.6 \pm 0.1$  eV (Fig. 5) between the 200 and 550°C reductions. The rhodium results are shown in Fig. 6. We found that after the initial reductions, when the catalysts were oxidized in oxygen at 350°C and then both reduced at 200°C, a binding energy near 307.1 eV was obtained, almost 0.4 eV lower than the initial 200°C reduction. Further oxidation–reduction cycles of the two catalysts showed

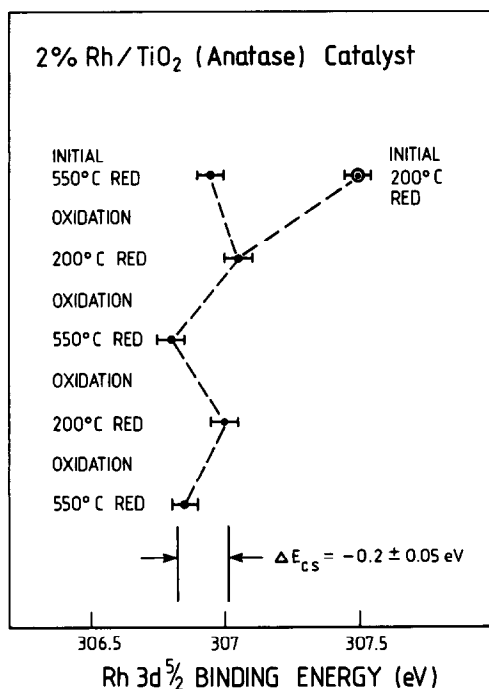


Fig. 6. Binding energies of the Rh 3d 5/2 peak on a 2% Rh/TiO<sub>2</sub> catalyst after several cycles of reduction and oxidation. Initially reduction at 200 and 550°C produces a large  $\Delta E_B = -0.6$  eV but this changes to  $-0.2$  eV after an oxidation–reduction cycle.

a reversible negative shift of  $-0.2 \pm 0.05$  eV between the 200 and 550°C temperatures. At 550°C the Rh 3d 5/2 binding energy decreased by 0.2 eV and after oxidation at 350°C and reduction at 200°C increased again by 0.2 eV. We interpret the initially high value of the 200°C reduction as the “nonannealed” state. After a high-temperature oxidation and further reduction at 200°C, the Rh particles increase in size to an average value which is maintained through further oxidation reductions. Changes in the binding energy of metal atoms due to different relaxation effects in different particles sizes are well documented (13). Since most of this effect may be observed in the very small particle size range (1–50 atoms), electron microscopy is not of much use in observing the sintering process. We did, however, measure the particle size of the 2% Rh/TiO<sub>2</sub> catalyst by electron microscopy after an initial reduction–oxidation–reduction cycle and found an average value of 1.5 nm (15 Å). This particular catalyst is therefore highly dispersed (>75%). As a concluding remark about the XPS results, it is clear that the initial binding energy difference between the low- and high-temperature reductions is not characteristic of a chemical shift but includes a large (0.4 eV for Rh/TiO<sub>2</sub>) relaxation energy difference. After annealing the catalyst several times the binding energy difference decreases to a reversible value of  $-0.2$  eV. We believe this value to be a lower limit on the chemical shift, as outlined in the discussion.

### 3.4 Surface Reduction of TiO<sub>2</sub> by Platinum

To check the validity of a mechanism involving the spillover of hydrogen from supported metal particles, and local reduction of the oxide surface, we attempted temperature-programmed reductions of Pt/TiO<sub>2</sub>. Three samples were prepared, a normal H<sub>2</sub>PtCl<sub>6</sub>/TiO<sub>2</sub> sample, pure TiO<sub>2</sub> powder, and platinum powder and TiO<sub>2</sub> ball-milled together in a homogeneous mixture. The

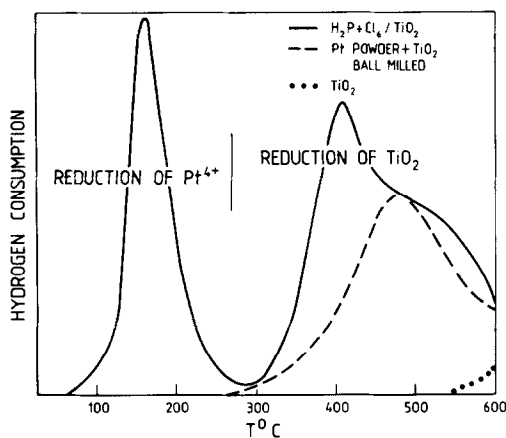


FIG. 7. Temperature-programmed reduction of  $\text{H}_2\text{PtCl}_6/\text{TiO}_2$  (1% Pt), 2% Pt- $\text{TiO}_2$  mixture (ball-milled), and pure  $\text{TiO}_2$ . The presence of Pt accelerates the reduction of  $\text{TiO}_2$  and moves the TPR peak from  $>550$  to  $400\text{--}500^\circ\text{C}$ , the same range where the SMSI effects are observed.

TPR results are shown in Fig. 7. For the normal unreduced  $\text{H}_2\text{PtCl}_6/\text{TiO}_2$  sample, two reduction peaks are seen near 160 and  $400\text{--}500^\circ\text{C}$ . For pure  $\text{TiO}_2$ , only a small amount of reduction occurs above  $550^\circ\text{C}$ . With Pt and  $\text{TiO}_2$  homogeneously mixed, a broad peak is found from 400 to  $600^\circ\text{C}$ .

The low-temperature peak ( $160^\circ\text{C}$ ) is due to  $\text{H}_2\text{PtCl}_6$  reduction and does not appear in the other two samples. The high-temperature reduction of pure  $\text{TiO}_2$  ( $>550^\circ\text{C}$ ) is considerably lowered in temperature by the addition of either small Pt particles ( $\text{H}_2\text{PtCl}_6$  case) or large Pt particles (ball-milled specimen). We interpret the high temperature peaks from 400 to  $500^\circ\text{C}$  as surface reduction of  $\text{TiO}_2$  to  $\text{TiO}_{2-x}$  by hydrogen spillover from the platinum particles adjacent to the  $\text{TiO}_2$  surface.

Although these results were only taken for platinum/ $\text{TiO}_2$  we would expect similar results for Rh/ $\text{TiO}_2$  and these metals on the other reducible oxides. With the formation of atomic hydrogen on the hot metal particles and spillover to the nearby oxide surface, the formation of reduced oxide cations is highly likely. Once the  $\text{Ti}^{3+}$  defects have interacted with the Pt particles, how-

ever, they will be oxidized to  $\text{Ti}^{4+}$  and detection with XPS would be very difficult. We have not been able to detect any significant concentration of  $\text{Ti}^{3+}$  on the Rh, Pt/ $\text{TiO}_2$  catalysts after  $550^\circ\text{C}$  reduction with XPS.

#### 4. DISCUSSION

XPS measurements of metal core level shifts by interaction of Pt and Ni with  $\text{SrTiO}_3$  surfaces have already been reported by Chung (6, 7). Chung *et al.* concluded that  $\text{Ti}^{3+}$  species donated electrons to Pt atoms and clusters, lowering the binding energies of the Pt 4f  $7/2$  level. In another study, Fung (9) has reported a negative 1.6 eV shift for the Pt 4f  $7/2$  level for a Pt/ $\text{TiO}_2$  film reduced in  $\text{H}_2$  at  $600^\circ\text{C}$ , relative to a sample which had received no reduction. Recently, Haller (8) has measured small negative binding energy shifts of 0.1–0.2 eV for Rh/ $\text{TiO}_2$  catalyst samples reduced at 200 and  $400\text{--}450^\circ\text{C}$ . Haller (8) also observed large initial splittings of the BEs (0.6 eV) for Rh/ $\text{TiO}_2$  which he attributed to a change in the particle size of the Rh clusters.

We are essentially in agreement with Haller (8). Fung's (9) value of  $-1.6$  eV is far too large to be due solely to electron transfer ( $\sim 1.5$  electrons per Pt atom!). His results may be explained by a difference in the particle size between the evaporated Pt/ $\text{TiO}_2$  film and the one sintered in  $\text{H}_2$  at  $600^\circ\text{C}$ , as mentioned in his paper (9).

Our results show clearly that the catalyst must be oxidized and reduced at least one cycle before a stable set of binding energies at 200 and  $550^\circ\text{C}$  are obtained. We then observe a small reversible  $-0.2$  eV shift indicating electron transfer to the Rh clusters. The results on the other catalysts (Pt/ $\text{TiO}_2$ , Rh/ $\text{Nb}_2\text{O}_5$ , Rh/ $\text{V}_2\text{O}_3$ ) also have a large initial splitting which is mostly due to a difference in particle size between the initially reduced catalysts. We did not repeat the Rh/ $\text{TiO}_2$  measurements on the other catalysts, but it is likely that only small reversible shifts would be observed on these as they are less highly dispersed than 2% Rh/ $\text{TiO}_2$ . As men-

tioned previously, the 2% Rh/TiO<sub>2</sub> catalyst had an average particle size of 1.5 nm (15 Å) as measured by electron microscopy (<75% dispersion). We believe that the high dispersion of this particular catalyst was responsible for the observation of the XPS chemical shifts, since most of the Rh atoms are surface atoms, and readily available for interaction with the reduced TiO<sub>2</sub> surface. Finally, the zero shift on Rh/Ta<sub>2</sub>O<sub>5</sub> is probably caused by the low surface area of Ta<sub>2</sub>O<sub>5</sub> and the consequent large particle size of supported Rh. We would not expect to see a chemical shift for large Rh particles.

The problem of separating the chemical shift due to electron transfer to metal atoms from the extra-atomic relaxation shift due to a change in metal atom environment is a difficult one. Chung (6) separated these two effects on a model Pt/SrTiO<sub>3</sub> catalyst by varying the amount of Pt on the SrTiO<sub>3</sub> surface and subtracting the relaxation shift from the total shift to get a chemical shift. Fung (9) was not able to separate the two effects on a Pt/TiO<sub>2</sub> film. Both our results and Haller's (8) eliminated the particle size effects by presintering the Rh/TiO<sub>2</sub> catalyst, and then comparing the shift with oxidation cycles in between each reduction.

One is still left to ask whether this 0.2 eV shift of the Rh 3d 5/2 peak represents purely electron transfer to rhodium or it is again a relaxation shift caused by a difference in the Rh environment or particle size at the two different reduction temperatures? This is a difficult question to answer, since it is quite possible that there is a change in dispersion or particle size of the rhodium clusters, between 200 and 550°C. If we assume that Tauster and Baker's (1-3) raft model is valid then the rhodium clusters would "flatten out" on the TiO<sub>2</sub> surface at 550°C and become spherical or bulk-like at 200°C reductions (provided there is an intervening oxidation cycle). As the number of rhodium neighbor atoms decreases, one would expect a positive (increasing binding energy) shift for the Rh core levels due to less extra-

atomic relaxation. Such a shift was observed by Chung for Pt/SrTiO<sub>3</sub> (0.8 eV for single atoms relative to a bulk environment). Other studies have shown binding energy shifts of ~1 eV for Pt core levels on a Pt/C substrate as the particle size was varied between single atoms and large clusters (14). Any positive binding energy shift caused by reduced extra-atomic relaxation would tend to offset the negative chemical shift caused by electron transfer. We feel that the -0.2 eV shift observed on the Rh/TiO<sub>2</sub> catalyst is a *lower limit* for the chemical shift and may include a substantial (~+0.5 eV) relaxation shift. In this case the actual chemical shift would be >-0.5 eV; a value more consistent with Horsley's (4) result of 0.6 e<sup>-</sup> per Pt atom. Since the chemical effects of high-temperature reduction on the catalysts are so dramatic, we feel that substantial electron transfer (>0.5 e<sup>-</sup> per atom) must occur from the support to rhodium or platinum. Our result of -0.2 eV for the Rh 3d 5/2 shift is consistent with substantial (>0.5 e<sup>-</sup> per Rh atom) electron transfer to rhodium *only* if there is an increase in the dispersion of the Rh at 550°C relative to 200°C.

The occurrence of Ti<sup>3+</sup> on TiO<sub>2</sub> surfaces is well documented, especially by sputtering experiments (10) and ESR investigations (11). The temperature-programmed reductions in Fig. 7 give additional support for hydrogen spillover as a mechanism for Ti<sup>3+</sup> formation on TiO<sub>2</sub>. Coupled with the ease of oxidation of the lower valence states on the oxide surfaces and the negative chemical shifts for Rh/TiO<sub>2</sub>, we feel there is substantial evidence to support the electron transfer theory. Further investigations need to be done into the effects of electron transfer into particles or clusters of varying sizes, and the correlation with reactivity measurements on these catalysts.

## 5. CONCLUSION

Of the Group IIIa-Va oxides studied, TiO<sub>2</sub>, V<sub>2</sub>O<sub>3</sub>, Ta<sub>2</sub>O<sub>5</sub>, and Nb<sub>2</sub>O<sub>5</sub> were found to undergo surface reduction in an ion beam



whereas  $\text{HfO}_2$  and  $\text{Y}_2\text{O}_3$  did not. The surface states formed on the reducible oxides were rapidly oxidized back to the stoichiometric composition by brief exposure to air. Such defect states ( $\text{Ti}^{3+}$ ,  $\text{V}^{2+}$ ,  $\text{Ta}^{2-4+}$ ,  $\text{Nb}^{2-4+}$ ) are probably the species responsible for the SMSI effect on oxides used as supports. Indirect evidence for SMSI effect was found by XPS measurements of core level shifts in Rh and Pt supported on the oxides. For one particular catalyst, 2% Rh/ $\text{TiO}_2$ , a large difference ( $-0.6 \pm 0.5$  eV) was observed for the Rh 3d 5/2 BE after initial reductions at 550°C compared with 200°C. Further oxidation and reduction cycles set a lower limit on the actual chemical shift due to electron transfer to rhodium as  $-0.2 \pm 0.05$  eV. Approximately 0.4 eV of the original difference was due to a change in the rhodium particle size after the first high-temperature heating cycle. Temperature-programmed reduction of Pt/ $\text{TiO}_2$  mixtures, pure  $\text{TiO}_2$  and unreduced  $\text{H}_2\text{PtCl}_6/\text{TiO}_2$  was shown to differentiate between metal reduction and  $\text{TiO}_2$  surface reduction. The presence of Pt metal particles was found to accelerate the reduction of  $\text{TiO}_2$  in the temperature range 400–500°C much lower

than the normal reduction temperature of  $>550^\circ\text{C}$ .

## REFERENCES

1. Tauster, S. J., Fung, S. C., and Garten, R. L., *J. Amer. Chem. Soc.* **100**, 170 (1978).
2. Tauster, S. J., and Fung, S. C., *J. Catal.* **55**, 29 (1978).
3. Baker, R. T. K., Prestridge, E. B., and Garten, R. L., *J. Catal.* **56**, 390 (1979).
4. Horsley, J. A., *J. Amer. Chem. Soc.* **101**, 2870 (1979).
5. "Handbook of X-Ray Photoelectron Spectroscopy." Perkin Elmer Corporation, 1979.
6. Bahl, M. K., Tsai, S. C., and Chung, Y. W., *Phys. Rev. B* **21**, 1344 (1980).
7. Kao, C. C., Tsai, S. C., Bahl, M. K., Chung, Y. W., and Lo, W. J., *Surf. Sci.* **95**, 1 (1980).
8. Chien, S. H., Shelimov, B. N., Resasco, D. E., Lee, E. H., and Haller, G. L., *J. Catal.* **77**, 301 (1982).
9. Fung, S. C., to be published.
10. Henrich, V. E., Dresselhaus, G., and Zeiger, H. J., *Phys. Rev. Lett.* **36**, 1335 (1976).
11. Hulzinga, T., and Prins, R., *J. Phys. Chem.* **85**, 2156 (1981).
12. Foger, K., to be published.
13. Takasu, Y., Unwin, R., Tesche, B., Bradshaw, A. M., and Grunze, M., *Surf. Sci.* **77**, 219 (1978).
14. Mason, M. G., Gerenser, L. J., and Lee, S. T., *Phys. Rev. Lett.* **39**, 288 (1977).
15. Henrich, V. E., *Progr. Surf. Sci.* **9**, 143 (1979).